General analytical treatment of the flow field relevant to the interpretation of passive fluxmeter measurements

Harald Klammler,[1,2,3] Kirk Hatfield,[1,2] Michael D. Annable,[2,4] Eugene Agyei,[1,2] Beth L. Parker,[5] John A. Cherry,[5] and P. S. C. Rao[6]

Received 8 November 2005; revised 4 July 2006; accepted 31 August 2006; published 5 April 2007.

[1] Relevant flow dynamics for the interpretation of passive fluxmeter (PFM) measurements are investigated by determining the properties of the flow field inside the PFM and its relationship to the undisturbed ambient fluxes in the aquifer. The flow domain is treated in two dimensions and consists of a system of concentric annular filter zones of different radii and hydraulic conductivities. Flow inside the PFM is shown to be uniform regardless of well configuration. Analytical expressions quantifying flow convergence are derived for an increasing number of rings, validated against numerical modeling and used to perform a sensitivity analysis. One of the derived convergence relationships is embedded in an inverse model to estimate aquifer and well screen conductivities and ambient groundwater and methyl-tertiary-butyl-ether (MTBE) fluxes in the Borden Aquifer under controlled flow conditions. Results compare well to independent estimates when the method of quantifying convergence is consistent with field conditions.

Citation: Klammler, H., K. Hatfield, M. D. Annable, E. Agyei, B. L. Parker, J. A. Cherry, and P. S. C. Rao (2007), General analytical treatment of the flow field relevant to the interpretation of passive fluxmeter measurements, *Water Resour. Res.*, *43*, W04407, doi:10.1029/2005WR004718.

1. Introduction

[2] Subsurface contaminant mass flows and fluxes are increasingly being viewed as critical information needed to address various elements of aquifer and groundwater remediation. These elements include: source prioritization, risk prediction, compliance monitoring, remediation endpoint evaluation, and contaminant attenuation assessment [*Einarson and Mackay*, 2001; *Schwarz et al.*, 1998; *U.S. Environmental Protection Agency*, 1998; *Rao et al.*, 2002; *Feenstra et al.*, 1996]. As a result of this increased interest in subsurface contaminant mass discharges and fluxes, various quantitative methods have been developed [*Borden et al.*, 1997; *Holder et al.*, 1998; *Schwarz et al.* 1998; *King et al.*, 1999; *Teutsch et al.*, 2000; *Kao and Wang*, 2001; *Bockelmann et al.*, 2001]. These methods assume the groundwater discharge is known or can be calculated from measured hydraulic gradients and assumed or measured aquifer hydraulic conductivities. Recently, *Hatfield et al.* [2004] introduced and *Annable et al.* [2005] field tested a new in situ method for the simultaneous measurement of both local groundwater specific discharge and local contaminant mass flux. This new method uses a downhole device known as a passive fluxmeter (PFM) which for certain well designs and under specific site conditions provides direct measures in the absence of data on the hydraulic gradient or the mean aquifer conductivity. Otherwise, the depth-averaged aquifer conductivity and the hydraulic gradient are needed for interpreting PFM measurements.

[3] The PFM is essentially a self-contained permeable unit that is inserted into a well or boring exactly fitting its diameter such that it intercepts groundwater flow but does not retain it. The interior composition of the PFM is a matrix of hydrophobic and hydrophilic permeable (e.g., granular) sorbents that retain dissolved organic and/or inorganic contaminants present in the fluid intercepted by the unit. The sorbent matrix is also impregnated with known amounts of one or more fluid soluble ''resident tracers''. These tracers are leached from the sorbent at rates proportional to fluid flux. After a specified period of exposure to groundwater flow, the PFM is removed from the monitoring well. The sorbent is extracted to quantify the mass of all contaminants intercepted by the PFM and the residual masses of all resident tracers. The extracted mass of each contaminant is used to calculate cumulative or time-averaged contaminant-specific mass flux, while residual resident tracer masses are used to calculate the cumulative or time-averaged groundwater specific discharge. Depth variations of both water and contaminant fluxes can be measured in an aquifer from a single PFM by vertically segmenting the exposed sorbent packing and analyzing each segment for

[1]Department of Civil and Coastal Engineering, University of Florida, Gainesville, Florida, USA.
[2]Inter-Disciplinary Program in Hydrologic Sciences, University of Florida, Gainesville, Florida, USA.
[3]Department of Hydraulic Structures and Water Resources Management, Graz University of Technology, Graz, Austria.
[4]Department of Environmental Engineering Sciences, University of Florida, Gainesville, Florida, USA.
[5]Department of Earth Sciences, University of Waterloo, Waterloo, Ontario, Canada.
[6]School of Civil Engineering, Purdue University, West Lafayette, Indiana, USA.

0043-1397/07/2005WR004718

resident tracers and contaminants. This segmenting may be achieved by the deployment of impermeable packers along the axis of the PFM, which additionally serve the purpose of minimizing vertical currents inside the PFM.

[4] In the course of interpreting the measured tracer and contaminant masses in terms of groundwater and contaminant fluxes, it is essential to know (1) the properties of the flow field inside the PFM in order to infer respective tracer elution (and contaminant retention) characteristics relating the detected tracer and contaminant masses to the respective fluxes inside the PFM, and (2) the relationship between those fluxes inside the PFM and the ambient fluxes in the undisturbed aquifer, which are the actual magnitudes of interest. The latter is generally quantified in a dimensionless flow convergence factor α (dimensionless). Neglecting the presence of a well screen and additional filter zones (e.g., a filter pack) and assuming reversible, linear and instantaneous tracer partitioning between water and PFM sorbent, *Hatfield et al.* [2004] determined a tracer elution characteristic as follows:

$$q_1 = \frac{2r\theta R_d \xi}{t} \tag{1}$$

where q_1 [L/T] is the water flow rate through the PFM, r [L] is the radius of the PFM cylinder, θ (dimensionless) is the water content in the sorbent, R_d (dimensionless) is the retardation of the tracer on the sorbent, and t [T] is the sampling duration. ξ is the dimensionless cumulative volume of water intercepted by the PFM [*Hatfield et al.*, 2002; *Annable et al.*, 2005] and is obtained iteratively using

$$\xi = \left\{ 1 - \left[\sin\left(\frac{\pi \Omega_R}{2} + \xi \sqrt{1-\xi^2} \right) \right]^2 \right\}^{1/2} \tag{2}$$

where Ω_R (dimensionless) is the relative mass of resident tracer retained in the PFM sorbent at the particular well depth following exposure to the groundwater flow field for duration t. Nonlinearities in the desorption of the resident tracers may as well be taken into account; however, special consideration must be given to the determination of R_d [*Hatfield et al.*, 2004].

[5] Equations (1) and (2) are based on the conclusion of *Strack and Haitjema* [1981] or *Wheatcraft and Winterberg* [1985] that the flow field inside a circular zone of contrasting hydraulic conductivity with respect to an otherwise homogeneous surrounding flow domain is uniform (provided a uniform far field). The flow convergence factor α is simply the ratio of flow inside the PFM to the ambient groundwater specific discharge. In this case, α equates to α_1 (dimensionless) [*Strack and Haitjema*, 1981; *Wheatcraft and Winterberg*, 1985]:

$$\alpha_1 = \frac{q_1}{q_0} = \frac{2}{1 + \frac{k_0}{k_1}} \tag{3}$$

where q_0 [L/T], is the undisturbed ambient groundwater flux, and k_1 [L/T] and k_0 [L/T] are the hydraulic conductivities of the PFM sorbent and the aquifer, respectively. Thus equations (1), (2), and (3) serve to determine the local ambient specific discharge q_0 in the aquifer for a given PFM segment.

[6] The time-averaged convective contaminant mass flux from a finite sampling duration is calculated from mass of contaminant intercepted by the PFM using the following equation [*Hatfield et al.*, 2004]:

$$J_C = \frac{1.67 m_C}{\alpha \pi r b t} \tag{4}$$

where J_c [M/(L^{2}T)] is the time-averaged ambient convective contaminant mass flux, m_c [M] is the mass of contaminant sorbed, b [L] is the length of sorptive matrix sampled or the vertical thickness of aquifer interval interrogated, and t [T] is the duration of the measurement. Here again, an appropriate estimate of α is needed to assess the local ambient contaminant flux associated with a PFM segment. The term "local" refers to the scale of groundwater and contaminant flux measurements within a control transect, and is defined here by the product $2r\alpha b$ representing the cross section of the aquifer interrogated by one PFM segment of length b.

[7] Because it is the ambient groundwater discharge q_0 and contaminant flux J_c we seek to measure, the effects of a well screen and possible filter rings on the flow field inside the PFM sorbent and on the flow convergence factor α, need to be quantified. To the best of our knowledge, flow distortion in this context has only been investigated for open wells and not from the perspective of a well containing a PFM. The most pertinent of such studies are those of *Ogilvi* [1958] and *Drost et al.* [1968] (or, equivalently, *Halevy et al.* [1967]), who give expressions for α_∞ (dimensionless) representing the flow convergence factor for an open well (an infinitely permeable PFM); in this case, they quantify α_∞ for a screened well and a screened well with a filter pack, respectively. While these expressions do not specify the exact properties of the flow field (e.g., streamlines) and cannot be used to describe flow through PFMs, they do possess a form which can be used to derive analytical expressions for the flow convergence factor of a PFM in a well. For example, it is shown later that equation (3) can be derived from *Ogilvi* [1958] and that the α factor for a PFM in a screened well results from the work of *Drost et al.* [1968].

[8] Analytical extensions of the work by *Drost et al.* [1968] that quantify α_∞ for open wells of different designs could be used to derive expressions for α of PFMs installed in those wells. *Bidaux and Tsang* [1991] introduced a general two-dimensional semianalytical approach in which the flow field around an open borehole or an impermeable cylinder is determined given a complex domain of radially variable hydraulic conductivity. Though the approach provided numerical flow solutions, it was also true but less obvious that the semianalytical method could also be used to generate analytical expressions of α_∞ for systems more complex than previously considered. Presumably, *Bidaux and Tsang* [1991] could have used the method to derive a generalized analytical expression for α_∞ for wells configured with multiple concentric homogeneous rings of varied media (i.e., screens, filter packs, and development zones); however, a personal communication led them to believe such a solution already existed. Instead, *Bidaux and Tsang* [1991] produced an explicit analytical solution for α_∞ (not for the entire flow field) for the particular case of

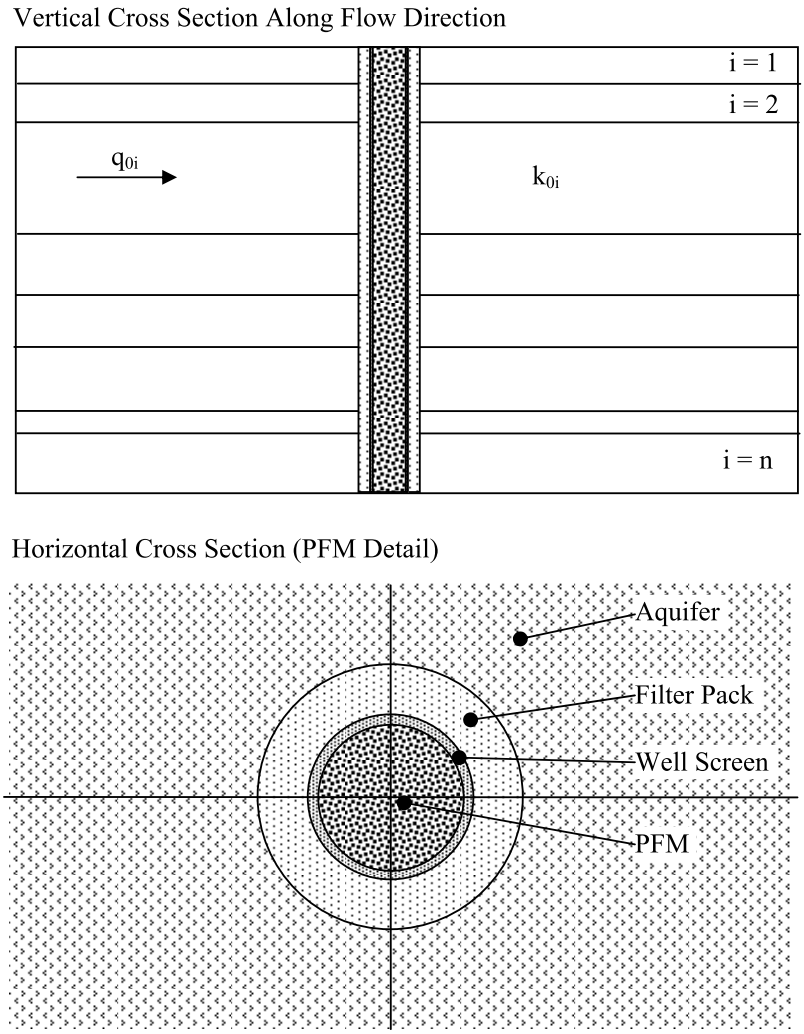

Figure 1. Vertical and horizontal cross sections of a possible monitoring well configuration with PFM installed in a perfectly multilayered aquifer.

hydraulic conductivity being an exponential function of radial distance from the well. However, as recognized by both authors and later *Palmer* [1993], this solution was of limited practical value due to uncertainties in the appropriateness of the adopted conductivity function as well as due to difficulties in the determination of function parameters. In more recent studies *Palmer* [1993] and *Kearl* [1997] did not use the semianalytical approach to derive desired expressions for α_∞ or generate required numerical simulations. Furthermore, they did not verify the existence of the general equation for α_∞ noted by *Bidaux and Tsang* [1991].

[9] Hence it is first observed that there are methods (analytical and semianalytical) for investigating the flow field and determining α_∞ for open wells; however, analytical extensions beyond *Drost et al.* [1968] have not been found in the literature except for the particular case discussed by *Bidaux and Tsang* [1991]. Second, no method can be identified that allows for a direct and fully analytical evaluation of the properties of the flow field inside a PFM installed in a monitoring well or that allows for the quantification of the pertinent flow convergence factor α.

[10] The present paper develops a flow field analogy that is used to determine the entire flow field through a system of an arbitrary number of concentric annular filter zones, thus providing direct solutions to the issues of interest discussed above. The flow field analogy relates the case of a uniform flow field disturbed by an impermeable (or infinitely permeable) circle and the case of a uniform flow field disturbed by a circular zone of contrasting hydraulic conductivity, which is neither zero nor infinite. The approach is fully analytical and does not require the adoption of any boundary conditions other than the uniformity of the far field, which, for practical field applications, is relaxed to the assumption of uniform flow conditions in the undisturbed aquifer at a local scale around the observation well (i.e., >10 times the well screen/filter pack radius). Each PFM sorbent, well screen, additional filter rings and the aquifer (again at a local scale around the well) are idealized as homogeneous continua of constant and isotropic hydraulic conductivities (see horizontal cross section in Figure 1); the flow problem is thus reduced to essentially horizontal flow in two dimensions. Under the scenario of a vertically heterogeneous aquifer hydraulic conductivity, the occurrence of vertical currents inside the monitoring well constituents is neglected and the system is divided into separate and independent horizontal layers. This is regarded

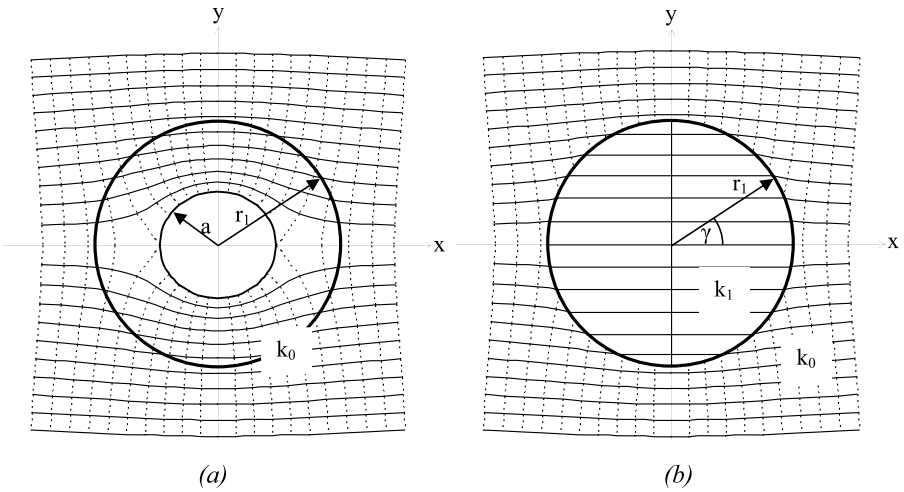

Figure 2. Analogy between (a) the flow around an impermeable circle and (b) the flow field with a circular inhomogeneity of conductivity k_1. The potential and stream functions along the circumference r_1 in Figures 2a and 2b are identical.

as a reasonable assumption especially for cases of a screened well without additional filter rings, since both the well screen and the PFM equipped with impermeable packers do not allow for significant currents along their vertical extents [*Annable et al.*, 2005]. The respective system is thus treated as a perfectly multilayered aquifer with homogeneous layers of conductivities k_{0i} [L/T] possessing a hydraulic gradient φ (dimensionless) independent of depth and horizontal flow q_{0i} [L/T] parallel to the layers (see vertical cross section in Figure 1). The results obtained are subjected to sensitivity analyses regarding uncertain parameters such as an aquifer or well screen hydraulic conductivity and they are validated against numerical simulations using finite difference methods. Finally, one of the derived convergence relationships is used to develop a general inverse approach for using PFM data to generate depth varying estimates of aquifer conductivities, groundwater specific discharge, and contaminant flux. The method is tested in a gated flow-controlled system placed in the Borden Aquifer.

2. Development and Application of the Relevant Flow Field Analogy

2.1. Uniform Flow Field Disturbed by an Impermeable Circle

[11] Among other methods that exist to calculate the flow field around an impermeable circle or toward a simple borehole in a uniform far field, the method of conformal mapping leads to an immediate result. The appropriate mapping function is [e.g., *Strack*, 1989; *Betz*, 1964]

$$\underline{\Omega}(\underline{z}) = \Phi + i\Psi = q_0\left(\underline{z} + \frac{\underline{a}^2}{\underline{z}}\right) \tag{5}$$

where the underscoring indicates complex variables. $\underline{\Omega} = \Phi + i\Psi$ is the complex potential (Φ being the potential function and Ψ the stream function; i is the imaginary unit), q_0 the specific discharge of the uniform far field, and $\underline{z} = x + iy = r \cdot e^{i\gamma}$ the complex Cartesian or polar coordinates in the physical plane as depicted in Figure 2. $\underline{a}$ [L] is the radius of the circle, where $\underline{a} = a$ is real for the flow around an impermeable circle, and $\underline{a} = ia$ is imaginary for the flow toward a borehole. Equation (5) (with the respective real or imaginary parameter $\underline{a}$) returns the value of the complex potential $\underline{\Omega}$ for both cases at any location $\underline{z}$ outside the circle. Thus, by finding the real and imaginary parts of $\underline{\Omega}$, the potential and the stream functions are obtained as

$$\Phi = q_0\left(r + \frac{a^2}{r}\right)\cos\gamma \tag{6}$$

$$\Psi = q_0\left(r - \frac{a^2}{r}\right)\sin\gamma \tag{7}$$

Using these equations, the flow field around an impermeable circle results as depicted in Figure 2a, where the continuous lines represent streamlines (Ψ = const.) and the dotted lines represent potential lines (Φ = const.). By using $\underline{a} = ia$ instead of a, the flow field toward a borehole is obtained, as previously mentioned. Inspection of equations (6) and (7) shows that both the potential and the stream function are rational functions of the radius r and simple cosine and sine functions of the argument γ of the polar coordinates.

2.2. Uniform Flow Field in a Homogeneous Circular Domain

[12] Knowing the boundary conditions of a homogeneous circular flow domain, e.g., the potential and/or the stream function along the circumference, the flow field inside the circle can be determined by various methods [e.g., *Betz*, 1964]. For our purposes it is sufficient to consider the simple case of a uniform flow field inside a circle as illustrated by the parallel streamlines inside the homogeneous circle in Figure 2b. By assigning the value zero to the streamline at $y = 0$ it can be seen that the stream function along the circumference is a function proportional to $\sin\gamma$. Knowing that the set of potential lines inside the circle is perpendicular to the set of streamlines and assigning the value zero to the potential line at $x = 0$, the potential function along the circumference is seen to behave like $\cos\gamma$. From this, the inverse conclusion can be drawn that whenever the stream function and the potential function

along a circumference are functions of $\sin\gamma$ and $\cos\gamma$, then the flow field inside the homogeneous circle is uniform.

2.3. Uniform Flow Field Disturbed by a Circular Inhomogeneity of Finite Conductivity Greater Than Zero

[13] Figure 2b illustrates this flow domain where the homogeneous circle of radius r_1 [L] and hydraulic conductivity k_1 [L/T] from above is located in an aquifer of conductivity k_0 [L/T]. In order to determine the corresponding flow field, advantage is taken of the final conclusions of the previous two paragraphs. As depicted in Figure 2a, it can be seen that the inside of circle of radius r_1 can be interchanged with a homogeneous circle of the same radius but a still unknown conductivity k_1 as in Figure 2b. In both cases ψ and Φ show the same qualitative behavior along the circumference (sine and cosine functions of γ). The quantitative behavior is conditioned by the continuity of flow between the two cases; this means that k_1 has to be adopted with respect to k_0 such that the total flow through both circles is the same. If this is done, the two circles show the same qualitative and quantitative behavior of ψ and Φ along their circumferences and, as a consequence, they can be interchanged without altering the flow field outside the circles. For Figure 2a it can be stated from equation (7) that the total flow through the half ring $a \le r \le r_1$ is $\psi_a = \psi(r_1, \pi/2)$.

$$\Psi_a = q_0 r_1 \left(1 - \frac{a^2}{r_1^2}\right) \tag{8}$$

For Figure 2b, $\psi_b = q_1 \cdot r_1$, where the uniform flux q_1 [L/T] inside the circle can be calculated from Darcy's law as shown in equation (9). The potential $\Phi \cdot k_1/k_0$ (with Φ from equation (2)) is used inside the circle to account for the discontinuity of conductivity while continuity of the hydraulic head is preserved across the circumference [*Strack*, 1989]. Furthermore, $\Delta s = r_1 \cdot \cos\gamma$ represents the length of a streamline from the circumference to $x = 0$.

$$\Psi_b = \frac{\Phi}{\Delta s}\frac{k_1}{k_0} r_1 = \frac{q_0\left(r_1 + \frac{a^2}{r_1}\right)\cos\alpha}{r_1\cos\alpha}\frac{k_1}{k_0} r_1 = q_0 r_1 \left(1 + \frac{a^2}{r_1^2}\right)\frac{k_1}{k_0} \tag{9}$$

Setting $\psi_a = \psi_b$ imposes continuity and gives the two equivalent expressions of equations (10) and (11) that describe the flow field analogy of Figure 2.

$$\frac{k_1}{k_0} = \frac{1 - \left(\frac{a}{r_1}\right)^2}{1 + \left(\frac{a}{r_1}\right)^2} \tag{10}$$

$$\left(\frac{a}{r_1}\right)^2 = \frac{1 - \frac{k_1}{k_0}}{1 + \frac{k_1}{k_0}} \tag{11}$$

An intuitive interpretation of equation (11) can be given as follows: If k_1 is equal to k_0, then a is zero and the flow domain is homogeneous. For $k_1 < k_0$ the flow field will partly diverge around the inhomogeneity and $\underline{a}$ will take a real value corresponding to the case of flow around an impermeable circle. As k_1 becomes smaller, a approaches r_1 and the flow divergence becomes more pronounced. Conversely, if $k_1 > k_0$, the flow will partly converge toward the inhomogeneity, resulting in an imaginary value for $\underline{a}$ as it is the case for flow toward a borehole. Again, as k_1 becomes larger, a approaches r_1 and the flow convergence becomes more significant. In other words, the analogy uses the flow field around an impermeable circle if $k_1 < k_0$ (as illustrated by Figure 2), and it uses the flow field toward an infinitely permeable circle (borehole) if $k_1 > k_0$. However, since we allow $\underline{a}$ to take real and imaginary values, these two cases are automatically included in the following derivations and do not have to be explicitly distinguished.

[14] In order to illustrate the application of the flow field analogy to solve the flow field for a given system of concentric filter rings, it is instructive to first demonstrate how such a system can be constructed using the analogy. Imagine a uniform flow field of strength q_0 at infinity in a domain of conductivity k_0 around an impermeable circle (Figure 3a). By applying the analogy of equation (10), the domain in some circle of radius $r_1 > a_0$ [L] can be substituted by a circular domain of homogeneous conductivity k_{1a} [L/T] (Figure 3b), keeping the flow field in the surrounding domain and, consequently, the stream function along the circumference unchanged. Next, the conductivity of the surrounding domain is changed from k_0 to k_1, while k_{1a} is maintained inside the circle. In order to also maintain the same flow field inside the circle (i.e., again maintain the same stream function along its circumference) the magnitude of the far field has to be changed from q_0 to q_1 to account for the different conductivity outside the circle (Figure 3c). In case k_0 and q_0 are ambient aquifer parameters, this step may be considered a temporary transformation that is reversed later. The resulting system consists of a circular inhomogeneity of conductivity k_{1a} in a flow domain of conductivity k_1 and a flux q_1 at infinity. Repeated application of the analogy (equation (11)) now converts the circle of conductivity k_{1a} into a system of an impermeable circle of radius a_1 [L] and a surrounding ring of conductivity k_1, which is the same conductivity as in the surrounding flow domain (Figure 3d). The resulting flow domain is seen to be qualitatively equivalent to the initial flow domain of Figure 3a leading to the possibility of a repeated application of equation (10) in order to arrive at the flow domain of Figure 3e, where, this time, the stream function along the circumference of radius $r_2 > a_1$ [L] remains unaffected. In summary, it is pointed out once more that the transformations performed above between Figures 3a and 3d do not alter the stream function along the circumference of radius r_1 while the transformation from Figure 3d to Figure 3e does not affect the stream function along the circumference of radius r_2. This fact allows for combining the initial flow field outside the circle of radius r_1 in a domain of conductivity k_0 and flux q_0 (Figure 3a) with the flow field inside the ring $r_2 < r < r_1$ of conductivity k_1 in Figure 3d and the flow field inside the circle of radius r_2 and conductivity $k_2 = k_{2a}$ [L/T] without the composite flow field (i.e., stream function) to become discontinuous. The flow field obtained corresponds to the system depicted in Figure 3f and it is seen that a continued application of equations (10) and (11) on the domain of Figure 3e allows for the addition of an arbitrary number of concentric filter rings.

3. Numerical Validation and Sensitivity Analysis

[15] A generalization of the above derivation to an arbitrary number of rings shows that the flow field in each filter ring in terms of the stream function can be described

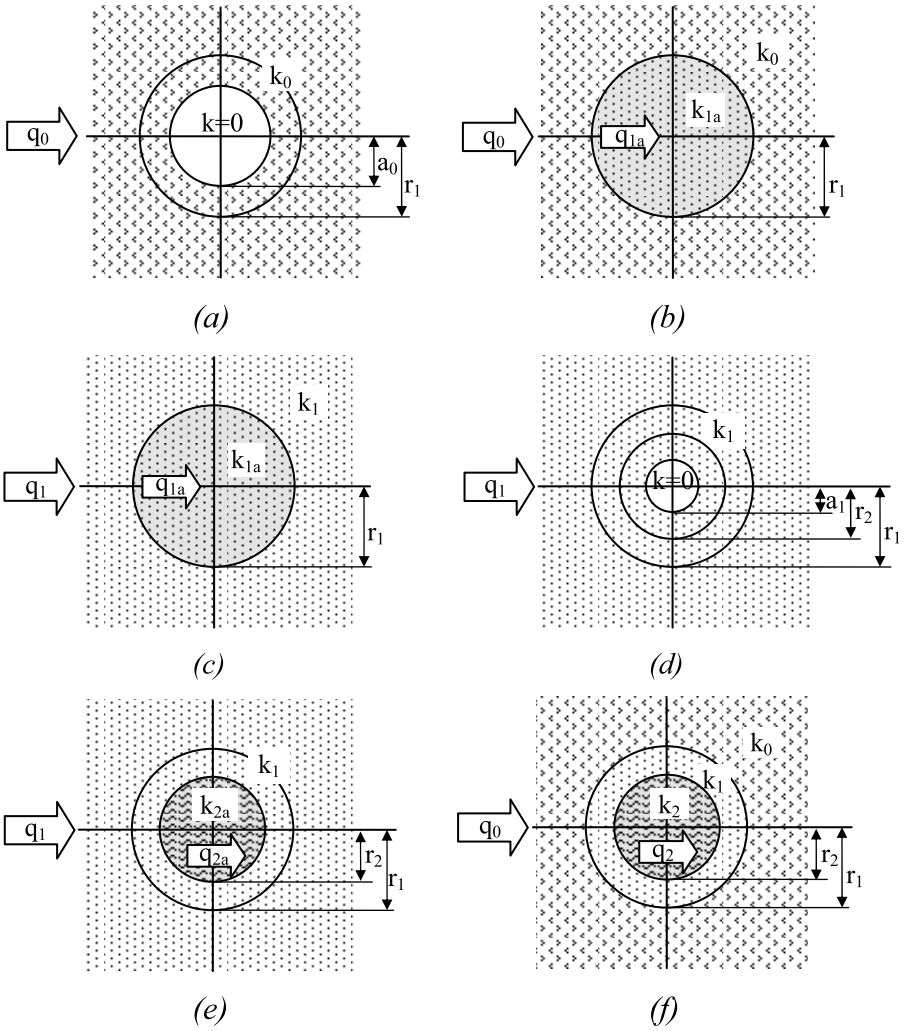

Figure 3. (a–f) Illustration of repeated application of the flow field analogy to construct a system of concentric filter rings.

by equation (7), where the parameters q and $\underline{a}$ have to be determined for each ring using the geometric and hydraulic properties of the composite flow domain. As a consequence of this observation, it is furthermore seen that $\underline{a}$ for the flow field in the center circle is zero leading to the expression of the stream function of a uniform flow field in equation (7), which is also confirmed by directly comparing Figures 3e and 2b. In other words, the flow field in the center circle, corresponding to the sorbent in the PFM context, is always uniform, independent of the number of filter rings, their radii and hydraulic conductivities. However, it is pointed out that this conclusion relies on the assumption of potential flow, which may not be accurate in the absence of a porous medium in the well, potentially resulting in a nonuniform flow field inside an open well [*Sekhar and Sano*, 2000]. For the PFM measurements, this result theoretically validates the assumption of a uniform flow field inside a PFM by *Hatfield et al.* [2004] and hence the applicability of equation (2) for cases where a well screen and other filter rings are present. In order to arrive at the flow convergence factors and the actual flow fields inside the filter rings for different well configurations, Appendix A gives an example of how to manipulate a given flow domain using equations (10) and (11) and how to arrive at the parameters q and a for each filter ring. In Appendix B the results of Appendix A are inspected and a general ad hoc formalism is derived to determine expressions for flow convergence factors for an arbitrary number of filter rings. Equations (12) and (13) represent resulting expressions for flow convergence factors for a PFM in a screened well (α_2 (dimensionless)) and in a screened well with a filter pack (α_3 (dimensionless)), respectively.

$$\alpha_2 = \frac{4}{\left(1+\frac{k_0}{k_1}\right)\left(1+\frac{k_1}{k_2}\right)+\left(1-\frac{k_0}{k_1}\right)\left(1-\frac{k_1}{k_2}\right)\left(\frac{r_2}{r_1}\right)^2} \tag{12}$$

$$\alpha_3 = \frac{8}{\left(1+\frac{k_0}{k_1}\right)\left(1+\frac{k_1}{k_2}\right)\left(1+\frac{k_2}{k_3}\right)+\left(1-\frac{k_0}{k_1}\right)\left(1-\frac{k_1}{k_2}\right)\left(1+\frac{k_2}{k_3}\right)\left(\frac{r_2}{r_1}\right)^2+\left(1+\frac{k_0}{k_1}\right)\left(1-\frac{k_1}{k_2}\right)\left(1-\frac{k_2}{k_3}\right)\left(\frac{r_3}{r_2}\right)^2+\left(1-\frac{k_0}{k_1}\right)\left(1+\frac{k_1}{k_2}\right)\left(1-\frac{k_2}{k_3}\right)\left(\frac{r_3}{r_1}\right)^2} \tag{13}$$

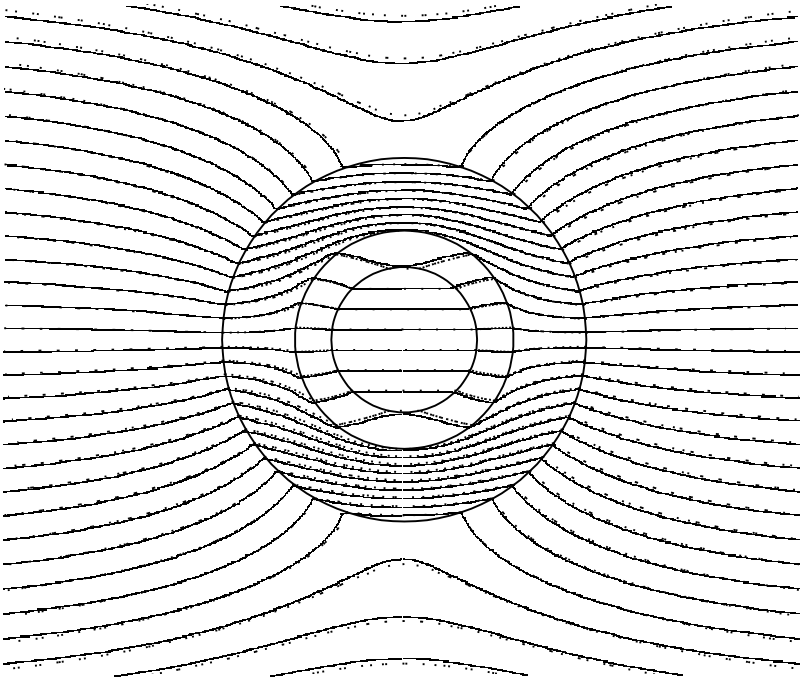

Figure 4. Comparison of streamlines in a borehole with well screen, filter pack, and PFM installed (r_1/r_3 = 2.5; r_2/r_3 = 1.5; k_3/k_0 = 100; k_2/k_0 = 40; k_1/k_0 = 200) from numerical simulation (solid lines) and flow field analogy (dotted lines).

The indexation of the conductivities starts with "0" in the aquifer and increases toward the center, while the indexation of the radii stars with "1" for the largest finite radius ($r_0 \rightarrow \infty$) and again increases toward the center of the filter rings as it is illustrated in Figure 3f. Thus, by letting k_2 in equation (12) and k_3 [L/T] in equation (13) approach infinity, *Ogilvi*'s [1958] and *Drost et al.*'s [1968] equations of the flow convergence factors $\alpha_{2\infty}$ (dimensionless) for open screened wells and $\alpha_{3\infty}$ (dimensionless) for open screened wells with a filter pack are obtained. In an analogous way, the flow convergence factor $\alpha_{4\infty}$ (dimensionless) for an open screened well with a filter pack and a developed filter zone in the aquifer as required by *Palmer* [1993] and *Kearl* [1997] is determined by deriving α_4 (dimensionless) from Appendix A or B and letting k_4 [L/T] approach infinity.

$$\alpha_{4\infty} = \frac{16}{D} \tag{14}$$

where D (dimensionless) is the denominator represented in Figure B1 using $k_4 \rightarrow \infty$.

[16] Figure 4 shows the streamlines through a possible configuration of a PFM installed in a screened well with a filter pack, where good agreement is seen between the continuous streamlines resulting from a high-resolution numerical solution using the finite difference method [*Harbaugh and McDonald*, 1996] and the dotted streamlines resulting from the application of the flow field analogy. A systematic comparison of flow fields using both methods for different well configurations and hydraulic conductivities ranging over several orders of magnitude was performed showing the same level of agreement as in Figure 4. This observation is also confirmed by the fact that the flow convergence factors computed from both methods present a maximum deviation at the second decimal, which is regarded in good agreement considering the restricted accuracy of numerical methods.

[17] Common observation well configurations include a well screen and the possible presence of a filter pack. A well development zone may be present as a result of the well construction or a particular well development process. However, no consistent method is currently available to infer the radial extent and the hydraulic properties of well development zones [*Bidaux and Tsang*, 1991]. As to the well screen and the filter pack the geometric parameters, i.e., radii of well screen and filter pack, can be determined with a relatively high accuracy compared to the hydraulic conductivities of these components. While the hydraulic conductivity of the PFM sorbent may as well be inferred relatively accurately from laboratory experiments, *Drost et al.* [1968] present a semianalytical approach to estimate the hydraulic conductivity of a well screen. Yet, the hydraulic conductivities of a well screen and particularly of an aquifer at a local scale around an observation well are often subject to uncertainties of up to orders of magnitude. As long as the filter rings may be regarded as homogeneous in their respective hydraulic conductivities these uncertainties do not affect the uniformity of the flow field inside the PFM sorbent. However, the flow convergence factor is influenced by uncertainties in the hydraulic conductivities, which motivates the performance of a sensitivity analysis of equations (12) and (13) with respect to these critical parameters.

[18] Propagating, for example, the individual random errors $\varepsilon(\cdot)$ of the hydraulic and geometric parameters (which are assumed to be pair wise uncorrelated) to the error $\varepsilon(\alpha_2)$

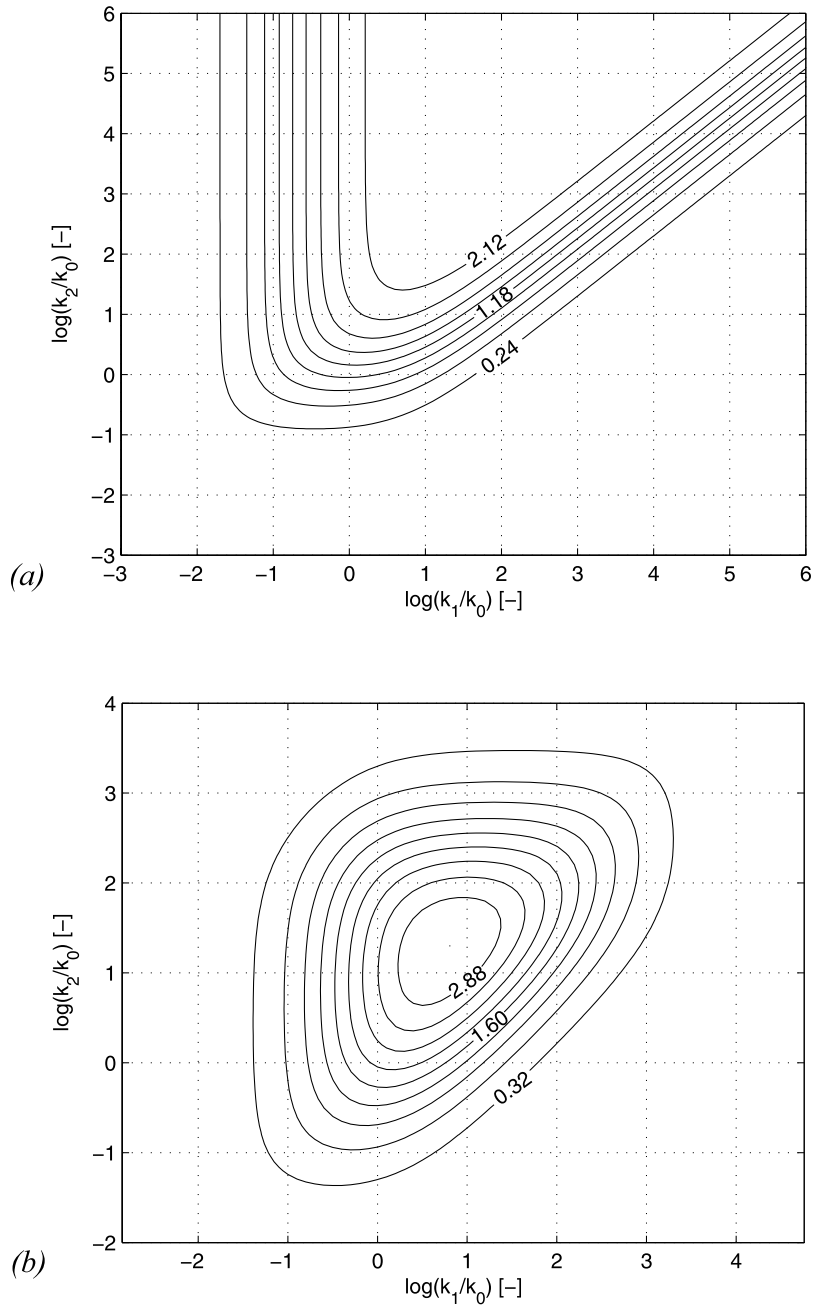

Figure 5. Examples of contour plots of (a) α_2 for a screened well ($r_1/r_2 = 1.2$) and (b) α_3 for a screened well with filter pack for qualitative sensitivity analysis.

of the flow convergence factor of a screened monitoring well leads to

$$\varepsilon(\alpha_2) = \sqrt{\left(\frac{\partial \alpha_2}{\partial k_0}\right)^2 \varepsilon(k_0)^2 + \left(\frac{\partial \alpha_2}{\partial k_1}\right)^2 \varepsilon(k_1)^2 + \left(\frac{\partial \alpha_2}{\partial k_2}\right)^2 \varepsilon(k_2)^2 + \left(\frac{\partial \alpha_2}{\partial r_D}\right)^2 \varepsilon(r_D)^2} \qquad (15)$$

where the partial derivatives are obtained from equation (12) and $r_D = r_2/r_1$ (dimensionless) is used. An analogous expression can be derived from equation (13) for the propagated error in α_3. Figures 5a and 5b represent examples of contour plots of α_2 and α_3, respectively, which graphically illustrate certain properties of the flow convergence factors.

[19] In general, from the structure of equations (12), (13), and (14), meeting the condition $k_{i+1} \gg k_i$, (i.e., providing for an increase in hydraulic conductivity by at least an order of magnitude for each filter ring going from the aquifer toward the PFM), maximizes α_i and minimizes the partial

derivatives $\partial\alpha_i/\partial k_i$ in the error propagation. Consequently, uncertainties in the hydraulic conductivities of the aquifer and well components present an insignificant effect on the flow convergence factor and α corresponds to the plateaus in the contour plots of Figure 5.

[20] In the particular case of a screened monitoring well and assuming well known aquifer and PFM conductivities k_0 and k_2, respectively, $\partial\alpha_2/\partial k_1$ is minimized by selecting a screen conductivity $k_1 = \sqrt{k_0 k_2}$. In another case where k_1 and k_2 are known to be reliably determined and k_0 is subject to uncertainties, then $k_1 \gg k_0$ minimizes $\partial\alpha_2/\partial k_0$; however, the additional constraint $k_2 > k_1/10$ (qualitatively inferred from Figure 5a) has to be met in order to assure a sufficient flux through the PFM (i.e., to avoid an extreme reduction of α below unity).

[21] Analogous considerations can be made for equation (13). Figure 5b shows a respective contour plot of the flow convergence factor for the configuration of Figure 4 where a filter pack is present and for different well screen (k_2) and filter pack (k_1) conductivities. It can be observed that both k_1 and k_2 may vary within approximately one order of magnitude around the peak value of the flow convergence factor without substantially affecting it. However, the presence of a filter pack (being the outmost ring) that is significantly more permeable than the aquifer implies the facilitation of vertical currents inside the filter pack, which may partially invalidate the measurement under heterogeneous conditions, in particular regarding the elaboration of a vertical flux profile. In the absence of a filter pack the outmost ring is represented by the well screen, whose vertical conductivity is zero (perforations are, in general, vertically not connected) and the problem of vertical currents is drastically reduced or eliminated. Impermeable packers along the PFM axis as mentioned in the initial section are used to mitigate vertical currents inside the PFM in order to approximately maintain two dimensional flow conditions.

[22] Hence, for PFM applications, an optimal observation well configuration can be identified as a screened well without a filter pack and a minimum alteration of the aquifer hydraulic properties in the surrounding of the well due to the well construction process (no well development). Using this configuration, equation (12) applies for the flow convergence factor, and meeting the condition $k_2 \gg k_1 \gg k_0$ assures a minimum uncertainty of the flow convergence factor even for significant uncertainties in the determination of the well screen and aquifer hydraulic conductivities. However, whenever the goal is to measure a depth averaged flux rather than a flux profile, then a highly permeable filter pack can be used to induce a physical averaging of the fluxes over depth (providing that short-circuiting of flow around PFM is avoided).

4. Field Application

[23] In practice, the insensitivity condition $k_2 \gg k_1 \gg k_0$ will not always be met, in particular when existing monitoring wells are used for PFM measurements. As a consequence, aquifer and well screen/filter pack conductivities need to be determined in order to allow for an adequate adjustment of the PFM measurements for flow convergence.

[24] In this section, a derived convergence relationship was applied to interpret ambient specific discharges and methyl-tertiary-butyl-ether (MTBE) fluxes from PFM measurements taken in a subsurface controlled flow gate installed in the Borden aquifer. The focus of the field test was to assess the efficacy of PFMs for measuring groundwater discharge and contaminant flux under controlled conditions. Two types of wells were tested: fully screened 5.1 cm wells and fully screened 5.1 cm wells with 2.5 cm filter packs. *Annable et al.* [2005] previously evaluated results from the field test using a forward model. Their key assumption was that flow convergence was vertically uniform in both well types. On the basis of this assumption, they made direct calculations of convergence factors using laboratory measured conductivities for aquifer material collected adjacent to the site and sample well screens. For flux interpretation, the method can boast the advantage of not needing a measured hydraulic gradient if aquifer and screen conductivities are known.

[25] A different approach is taken here, whereby data on the hydraulic gradient and the depth-averaged aquifer conductivity are combined with unadjusted PFM measurements of groundwater discharge and then used in an inverse model to generate depth varying estimates of conductivity for both the aquifer and the well. On the basis of these conductivities, depth varying convergence factors are calculated for final determination of ambient water and contaminant fluxes. This new approach represents an improvement over previous forward methods [*Annable et al.*, 2005; *Hatfield et al.*, 2004] because it is generally adaptable to all well designs, uses easily acquired data (gradients and depth-averaged aquifer conductivities) and returns unique estimates of depth varying aquifer conductivities, water fluxes, and contaminant fluxes. Results of testing this new approach in the field are compared to those of *Annable et al.* [2005] and to independent measurements and calculations.

4.1. Experiment

[26] Recognizing that the field experiment has been described elsewhere [*Annable et al.*, 2005], only the most pertinent information was reproduced here for the reader's convenience. Field testing was conducted in a subsurface controlled flow facility (gate 2) located at CFB Borden, Ontario, Canada [*Devlin et al.*, 2002]. Gate 2 was 24 m long and 2 ± 0.06 m wide and constructed with sheet pile keyed into the aquitard ~3.0 m below ground surface (in this paper the estimated standard error follows the ± symbol). At the closed end of the gate, a fully screened 5.1 cm extraction well was used to create steady groundwater flow in the channel. As illustrated in Figure 6, the gate contained three sampling transects situated 1 m apart. Three multilevel samplers (MLS) comprised the first transect, each equipped with 15 sampling ports spaced at 15 cm intervals. The second transect included three 5.1 cm fully screened PVC wells (designated FA wells). The third and final transect contained three 5.1 cm fully screened PVC wells each constructed with 2.5 cm filter pack (mean grain diameter 2.0 mm) (designated FB wells). Previous experiments left groundwater in the gate contaminated with MTBE [*Barker et al.*, 2000].

[27] Both water and MTBE fluxes were measured using PFMs installed in wells. MTBE concentrations were measured from MLS and from open FA and FB wells prior to PFM installation (see Table 1). During the experiment, the average discharge rate of the extraction well was 203 ± 2.3 mL/min

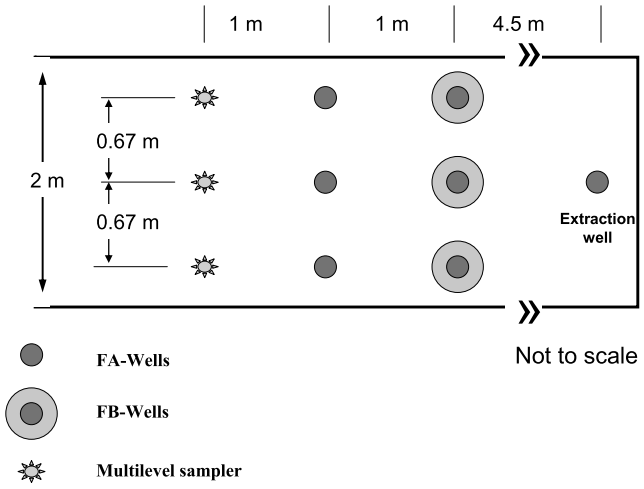

Figure 6. Plan view of the subsurface controlled flow gate at the Borden site.

which produced a measured hydraulic gradient of 0.016 ± 0.001; this gradient was determined from head measurements taken from 5 wells spaced over 22 m. The estimated saturated thickness of the aquifer was 174 ± 10 cm; this included 139 cm measured below the phreatic surface and 35 cm of estimated capillary fringe [*Xie*, 1994]. On the basis of the above stated gate width, the calculated saturated flow area was $3.5 \pm 0.2\ m^2$. Slug tests were conducted in the FA and FB wells at end of the experiment which produced an estimated depth-averaged aquifer conductivity of $\overline{k_O} = 5.1 \pm 1.0$ m/d.

4.2. General Inverse Model for Aquifer and Screen/Filter Hydraulic Conductivities

[28] One or more PFMs installed in a well generate depth varying measures of horizontal water and contaminant fluxes from n discrete vertical intervals along the well axis. At any arbitrary depth interval i, it can be assumed the local flow convergence satisfies equation (12) such that $\alpha_i = \alpha_{2i}$. Hence, at depth interval i the measured specific discharge through a PFM q_{2i}, is related to the unknown local ambient groundwater flux q_{0i} as shown in the following equation:

$$q_{2i} = \alpha_{2i} q_{0i} = \frac{4k_{0i}\varphi}{\left(1+\frac{k_{0i}}{k_{1i}}\right)\left(1+\frac{k_{1i}}{k_2}\right)+\left(1-\frac{k_{0i}}{k_{1i}}\right)\left(1-\frac{k_{1i}}{k_2}\right)\left(\frac{r_2}{r_1}\right)^2} \quad \forall i = 1,2,\ldots,n \tag{16}$$

where φ (dimensionless) is the hydraulic gradient; k_2 is the hydraulic conductivity of the PFM; k_{0i} is the unknown local conductivity of the aquifer at interval i; k_{1i} is the unknown local conductivity of the well (screen or screen–filter pack) at interval i; and the ratio r_2/r_1 is 0.8 and 0.5 for the FA and FB wells respectively. Using the same sampling intervals, the depth-averaged aquifer conductivity $\overline{k_0}$ is calculated as follows:

$$\frac{\sum_{i=1}^{n} z_i k_{0_i}}{\sum_{i=1}^{n} z_i} = \overline{k_0} \tag{17}$$

in which z_i is the of length sample interval i along the PFM axis.

[29] The most general formulation of the inverse model is obtained by combining equations (16) and (17). Assuming $\overline{k_0}$ is known a priori, (16) and (17) constitute a system of $n + 1$ equations composed of 2n unknown well and aquifer conductivities. To solve this system of equations for unique estimates of k_{0i} and k_{1i} ($\forall i$ = 1, 2, …, n) assumptions are made to reduce the total number of unknowns to equal the number of equations. These assumptions vary with well design.

4.3. Inverse Modeling of Simple Screened Wells

[30] For purposes of analyzing PFM data derived from simple screened wells (i.e., the FA wells), it is assumed the aquifer medium and well screen are in intimate contact (i.e., no annulus), and that the local well screen conductivity k_{1i} is a simple linear function of the local aquifer conductivity k_{0i}.

$$k_{1i} = \gamma k_{0i} \quad (\forall i = 1,2,\ldots,n) \tag{18}$$

and

$$\gamma \approx \Gamma f_A \quad (\forall i = 1,2,\ldots,n) \tag{19}$$

where γ is assumed proportional to the fraction of open area in the well screen f_A, and the coefficient Γ, which accounts for the increased porosity and permeability of granular medium adjacent to the wall of the screen [*Dudgeon*, 1967]. Combining (16)–(18) produces a simplified inverse model. The resultant system of $n + 1$ equations, composed of an equal number of unknowns, can be solved for unique estimates of γ and the local aquifer conductivity at each depth interval. Local estimates of the screen conductivity are subsequently estimated through equation (18). Further inspection of the model shows local flow convergence will be defined by γ alone, wherever the PFM conductivity is much greater than the local screen conductivity. Moreover, if $k_2 \gg k_{1i}$ ($\forall i$ = 1, 2, …, n), flow convergence will be depth-uniform.

[31] Listed in Table 2, for multiple elevations above the Borden aquitard, are unadjusted PFM measurements of both water and MTBE fluxes from FA wells. Also listed are inverse estimated aquifer and screen conductivities. Predicted conductivities reflect measured values of 5.1 m/d and 0.016 assigned respectively to parameters $\overline{k_0}$ and φ in the model. A PFM conductivity of 330 m/d [*Annable et al.*, 2005] and equation (12) are required to reproduce listed flow convergence factors. Ambient fluxes presented in the last two columns of Table 2 are calculated from the unadjusted measurements using theses α values. Table 3 lists gate-averaged values for γ and system conductivities

Table 1. Depth-Averaged MTBE Concentrations From MLS and PFM Wells[a]

Zone	MLS 16 Aug 2002	MLS 13 Aug 2002	FA Wells 13 Aug 2002	FB Wells 13 Aug 2002
1	2.14 ± 0.73	2.69 ± 0.82	2.36 ± 0.07	4.45 ± 0.13
2	2.16 ± 0.80	3.03 ± 1.03	2.79 ± 0.08	6.94 ± 0.20
3	1.29 ± 0.57	2.82 ± 1.23	2.37 ± 0.07	5.95 ± 0.17

[a]Plus/minus standard error. Units are mg/L.

Table 2. PFM Results of Screened Wells Without Filter Pack (FA Wells)

Well	Midpoint Elevation Above Aquitard, cm	q_2, [a] cm/d	MTBE J_2, [a] g/(m^2 d)	k_0, m/d	k_1, [b] m/d	α	q_0, cm/d	MTBE J_0, g/(m^2 d)
FA1	9	5.7	0.03	4.1	0.5	0.88	6.5	0.03
FA1	27	10.2	0.06	7.3	0.9	0.88	11.5	0.07
FA1	47	7.0	0.07	5.0	0.6	0.88	8.0	0.08
FA1	64	7.1	0.03	5.1	0.6	0.88	8.1	0.03
FA1	81	6.5	0.04	4.7	0.6	0.88	7.4	0.05
FA1	98	6.7	0.11	4.8	0.6	0.88	7.6	0.13
FA1	116	14.4	0.44	10.4	1.3	0.88	16.4	0.50
FA1	138	6.9	0.38	4.9	0.6	0.88	7.8	0.43
FA2	8	5.1	0.05	3.7	0.5	0.88	5.8	0.06
FA2	24	6.7	0.05	4.8	0.6	0.88	7.6	0.06
FA2	39	6.0	0.05	4.3	0.5	0.88	6.8	0.06
FA2	54	5.5	0.04	3.9	0.5	0.88	6.2	0.05
FA2	70	5.9	0.04	4.2	0.5	0.88	6.7	0.05
FA2	88	6.0	0.06	4.3	0.5	0.88	6.8	0.07
FA2	106	6.1	0.08	4.4	0.5	0.88	7.0	0.09
FA2	125	10.5	0.78	7.6	1.0	0.88	12.0	0.89
FA2	144	5.7	0.25	4.1	0.5	0.88	6.4	0.28
FA3	9	6.1	0.05	4.4	0.6	0.88	7.0	0.06
FA3	28	13.3	0.03	9.6	1.2	0.88	15.1	0.03
FA3	47	6.5	0.02	4.6	0.6	0.88	7.3	0.02
FA3	65	5.7	0.04	4.1	0.5	0.88	6.5	0.05
FA3	84	6.0	0.04	4.3	0.5	0.88	6.9	0.05
FA3	103	5.9	0.10	4.2	0.5	0.88	6.7	0.11
FA3	122	7.8	0.18	5.6	0.7	0.88	8.9	0.20
FA3	141	4.7	0.42	3.4	0.4	0.88	5.3	0.48
Average		7.1	0.14	5.1	0.6	0.88	8.1	0.16
Coefficient of variation		0.3	1.3	0.3	0.3	0.0	0.3	1.3

[a]Unadjusted measure by PFM.
[b]From equation (18) and inverse estimated $\gamma = 0.13$.

obtained by inverse modeling and resultant ambient water and MTBE fluxes. For comparison, analogous results are listed from independent sources/calculations and from a previous study [*Annable et al.*, 2005]. Results from the latter are based on a forward modeling analyses of the same unadjusted PFM data found in Table 2; and they appear in Table 3 as reported by *Annable et al.* [2005] or as quantities adjusted to reflect consistent flux units.

Table 3. Comparison of Fluxes and Conductivities Measured by PFM to Independent Estimates

	Annable et al. [2005]		This Study		
	FA Wells[a]	FB Wells[a]	FA Wells[a]	FB Wells[a]	Independent Estimates[a]
$\overline{k_O}$, m/d	17.0 ± 1.2	17.0 ± 1.2	5.1 ± 0.4	5.1 ± 0.6	5.2 ± 0.4[b]
$\overline{k_O}$, m/d	17.0 ± 1.2	17.0 ± 1.2	5.1 ± 0.4	5.1 ± 0.6	5.3 ± 0.4[b]
$\overline{k_O}$, m/d	17.0 ± 1.2	17.0 ± 1.2	5.1 ± 0.4	5.1 ± 0.6	4.9 ± 0.2[c]
$\overline{k_O}$, m/d	17.0 ± 1.2	17.0 ± 1.2	5.1 ± 0.4	5.1 ± 0.6	5.0 ± 0.2[c]
$\overline{k_O}$, m/d	17.0 ± 1.2	17.0 ± 1.2	5.1 ± 0.4	5.1 ± 0.6	5.3 ± 0.5[d]
$\overline{k_1}$, m/d	2.0 ± 0.2		0.6 ± 0.1		0.4[e] – 2.0[f]
$\overline{k_1}$, m/d		3.4 ± 0.3		2.6[g]	-
γ	0.12 ± 0.01[h]	-	0.13[d]	-	0.12 ± 0.02[i]
q_O, cm/d	8.7 ± 0.7	9.5 ± 0.7	8.1 ± 0.6	8.1 ± 0.9	8.4 ± 0.5[j]
J_O, g/m^2/d	0.17 ± 0.04	-	0.16 ± 0.06	-	0.16 ± 04[k]
J_O, g/m^2/d	-	0.42 ± 0.05	-	0.29 ± 0.04	0.31 ± 0.04[l]

[a]Plus/minus standard error.
[b]Core tests [*Labaky*, 2004].
[c]Slug tests [*Labaky*, 2004].
[d]From assuming a flow area of 3.5 ± 0.2 m^2, a total measured discharge of 202.6 ± 2.3 mL/min, and a measured hydraulic gradient of 0.016 ± 0.001.
[e]*Harlemann et al.* [1963], assuming spherical grains 0.025 cm in diameter occluding well screen slits.
[f]*Harlemann et al.* [1963], assuming a well screen free of sediment.
[g]Single-valued output from the inverse model.
[h]Calculated from ratio of $\overline{k_1}$ / $\overline{k_1}$.
[i]Equation (19), assuming $f_A = 0.06 \pm 0.01$ and $\Gamma = 2.0$.
[j]From assuming a flow area of 3.5 ± 0.2 m^2 and a total measured discharge of 202.6 ± 2.3 mL/min.
[k]From the calculated specific discharge (8.4 ± 0.5 cm/d) and a depth-averaged MTBE concentration from MLS (16 August 2002).
[l]From the calculated specific discharge (8.4 ± 0.5 cm/d) and a mean MTBE concentration derived from averaging the six open FA and FB well measurements (13 August 2002) and the three depth-averaged concentrations from MLS (3 August 2002).

[32] The independent assessments of water and contaminant flux, listed in Table 3, were predicated on the above calculated saturated flow area of 3.5 ± 0.2 m^2. Because PFMs generate direct measures of flux, no assumptions regarding flow area were needed. Gate-averaged ambient specific discharge and MTBE flux derived from inverse modeling were within 5% of independent estimates of 8.4 ± 0.5 cm/d for water and 0.16 ± 04 $g/m^2/d$ for MTBE. In addition, these fluxes were either close or indistinguishable from those reported by *Annable et al.* [2005]. Given the scale of this experiment, the high density of MLS and PFM sampling (particularly along vertical), and the relative homogeneity of the Borden aquifer, it was reasonable to expect agreement between independent and PFM estimates of MTBE fluxes, if the unadjusted PFM fluxes were properly processed to give accurate ambient fluxes [*Kubert and Finkel*, 2006].

[33] The close agreement between flux results derived from inverse estimated conductivities and those of *Annable et al.* [2005] stood in stark contrast to significant differences observed for predicted aquifer and screen conductivities. Inverse estimated aquifer conductivities ranged from 3.4 to 10.4 m/d but gave a depth-averaged value of 5.1 ± 0.4 m/d. This latter result was a direct consequence of equation (17). *Labaky* [2004] reported for the same gate, similar independent measures of depth-averaged aquifer conductivity from core (5.2 ± 0.4 and 5.3 ± 0.4 m/d) and slug tests (4.9 ± 0.2 and 5.0 ± 0.2 m/d). The aquifer conductivity reported by *Annable et al.* [2005] was based on laboratory tests and was three times larger than all other assessments (see Table 3). Differences in scale of measures taken in a well as opposed to smaller laboratory samples could explain this discrepancy.

[34] Resultant inverse estimated well screen conductivities averaged 0.6 ± 0.1 m/d and ranged from 0.4 to 1.3 m/d. The lower range was comparable with 0.4 m/d calculated using an empirical formula from *Harlemann et al.* [1963] and assuming spherical grains 0.025 cm in diameter occluded screen slits. An upper limit of 2.0 m/d was calculated using the same formula but assuming the screen was free of sediment. *Annable et al.* [2005] presented a novel laboratory method for measuring screen conductivities under ''well-like'' conditions using the above measured sample aquifer material. They found conductivities to be two to three times larger or 2.0 ± 0.2 m/d.

[35] The PFMs used in this study possessed a much greater conductivity than the aquifer or well screen. For simple screened wells (i.e., FA wells), this would induce uniform flow convergence which would depend more on the conductivity ratio γ, and less so on actual aquifer and well screen conductivities. The inverse model predicted a uniform flow convergence factor of 0.88 under a γ value of 0.13 (see Table 2). *Annable et al.* [2005] had assumed a constant flow convergence at the outset of their analysis, and so it would appear the inverse model confirmed their assumption. Taking the ratio of what they measured for screen and aquifer conductivities produced a γ value of 0.12 ± 0.01 and in turn a comparable convergence factor of 0.83 ± .07 (see Table 3). Thus flux results derived from the inverse model matched those reported by *Annable et al.* [2005] because (1) site conditions supported the assumption that α was uniform and (2) both methods independently obtained similar values for γ. Had the former not been true, the inverse model would have estimated different fluxes. To obtain yet another independent calculation of γ that might provide for broader validation of all methods, equation (19) was used. Following *Dudgeon* [1967] and specifying $\Gamma = 2.0$ and f_A to a measured value of 0.06 ± 0.01, the determined value of γ was again approximately 0.12 ± 0.02. This finding would appear to validate both the inverse model, and a simple approach of calculating γ through laboratory measured conductivities.

[36] The above analysis shows there are two available options for evaluating PFM measurements from simple screened wells. The first option is the inverse model, which is the most general. This method is the only alternative when site conditions suggest α is nonuniform and when f_A or γ cannot be estimated a priori (i.e., with existing wells). The model requires unadjusted PFM measures of water flux and data on the depth-averaged aquifer conductivity and the hydraulic gradient; but it returns estimates of depth varying aquifer conductivities, from which depth varying convergence factors and ambient water and contaminant fluxes are determined.

[37] The second approach, first presented by *Annable et al.* [2005], is only valid when site conditions support uniform flow convergence. This method requires prior assessments of f_A or γ (i.e., data generally available as new wells are installed). A measured hydraulic gradient is not required, and if f_A is known, equation (19) can be used to estimate γ without measured aquifer or screen conductivities. This simple method returns an estimate of α and depth varying estimates of ambient water and contaminant fluxes. The method does not predict depth varying aquifer conductivities. Such predictions require measured hydraulic gradients or depth-averaged aquifer conductivities.

4.4. Inverse Modeling of Screened Wells With Filter Packs

[38] To facilitate analysis of PFM data derived from screened wells with filter packs (i.e., the FB wells), the general inverse model is again simplified but under different assumptions. It is assumed the well screen and the filter pack are a single filter zone of depth-uniform effective conductivity k_1. Thus $k_1 = k_{1i}$ ($\forall i = 1, 2, \ldots, n$) such that combining (16) and (17) produces a system of $n + 1$ equations and again $n + 1$ unknowns. The resultant system of equations is solved for the effective well conductivity k_1 and again at each depth interval the local aquifer conductivity k_{0i}. Thus, for stratified aquifers the model predicts depth varying aquifer conductivities and convergence factors. Conditions giving exception are homogeneous aquifers and sites where $k_1 \gg k_{0i}$ ($\forall i = 1, 2, \ldots, n$). These conditions are not relevant here.

[39] Listed in Table 4, for multiple elevations above the Borden aquitard, are unadjusted PFM measurements of both water and MTBE fluxes from the FB wells and associated inverse model results. Modeling produced unique determinations for the effective uniform conductivity of the screen–filter pack k_1, and the local aquifer conductivity at each depth interval. Estimated local aquifer conductivities ranged from 2.1 to 13.8 m/d. This was broader than seen with the FA wells but again averaging 5.1 ± 0.6 m/d (see Table 3). The predicted screen/filter pack conductivity was 2.6 m/d versus 3.4 m/d estimated by *Annable et al.* [2005].

Table 4. PFM Results of Screened Wells With Filter Pack (FB Wells)

Well	Midpoint Elevation Above Aquitard, cm	q_2, [a] cm/d	MTBE J_2, [a] g/(m^{2}d)	k_0, m/d	k_1, m/d	α	q_0, cm/d	MTBE J_0, g/(m^{2}d)
FB1	8	8.7	0.23	2.9	2.6	1.92	4.5	0.12
FB1	24	16.6	0.13	13.8	2.6	0.76	21.9	0.17
FB1	39	13.2	0.34	6.6	2.6	1.27	10.4	0.27
FB1	54	12.3	0.20	5.5	2.6	1.40	8.8	0.14
FB1	70	14.6	0.32	8.7	2.6	1.06	13.8	0.30
FB1	88	7.2	0.58	2.1	2.6	2.13	3.4	0.27
FB1	105	8.5	1.02	2.8	2.6	1.95	4.4	0.52
FB2	9	10.8	0.15	4.3	2.6	1.61	6.7	0.10
FB2	28	12.1	0.21	5.4	2.6	1.42	8.6	0.15
FB2	47	11.5	0.41	4.9	2.6	1.50	7.7	0.27
FB2	65	12.8	0.52	6.1	2.6	1.32	9.7	0.39
FB2	84	14.4	0.53	8.4	2.6	1.09	13.2	0.48
FB2	103	7.9	0.58	2.5	2.6	2.03	3.9	0.28
FB2	122	12.4	1.26	5.7	2.6	1.38	9.0	0.91
FB3	9	12.3	0.12	5.6	2.6	1.39	8.8	0.09
FB3	27	12.5	0.37	5.8	2.6	1.36	9.2	0.27
FB3	47	10.0	0.46	3.7	2.6	1.73	5.8	0.27
FB3	64	10.0	0.42	3.7	2.6	1.72	5.8	0.24
FB3	81	9.8	0.55	3.5	2.6	1.76	5.6	0.31
FB3	98	8.7	0.48	2.9	2.6	1.91	4.6	0.25
FB3	116	8.0	0.72	2.5	2.6	2.01	4.0	0.36
Average		11.2	0.45	5.1	2.6	1.6	8.1	0.29
Coefficient of Variation		0.2	0.62	0.5	0.0	0.23	0.5	0.62

[a]Unadjusted measure by PFM.

Resultant convergence factors ranged from 0.76 to 2.03 and gave a depth-averaged value of 1.6 ± 0.1.

[40] Subsequent evaluation of ambient water and contaminant fluxes using inverse estimated system conductivities produced gate-averaged fluxes which were within 5% of independent estimates for water, 8.4 ± 0.5 cm/d and for MTBE, 0.31 ± 0.04 g/m^2/d. *Annable et al.* [2005] assumed flow convergence was constant and applied an $\alpha = 1.05$; this produced gate-averaged water and contaminant fluxes which were 13% and 35% greater than corresponding independent estimates (see Table 3). These larger discrepancies were believed to be a consequence of assuming a constant α for the FB wells when site conditions did not support this assumption. This would suggest further that forward modeling could dampen variations in estimated fluxes.

[41] Thus inverse modeling is recommended for the analysis of PFM data generated from screened wells equipped with filter packs. This requires additional measures of hydraulic gradients and depth-averaged aquifer conductivities; however, the outcome is an improved characterization of depth-varying aquifer conductivities and fluxes.

5. Summary

[42] The passive fluxmeter (PFM) is a permeable device installed in a monitoring well to deliver direct and simultaneous measures of local cumulative groundwater and contaminant mass fluxes in porous aquifers. The flow dynamics of the resulting system (aquifer, observation well, PFM) has to be determined in order to correctly interpret measurements by knowing the properties of the flow field inside the PFM sorbent and knowing the relationship between the measured fluxes inside the PFM sorbent and the undisturbed ambient fluxes in the aquifer. Previous approaches presented by *Drost et al.* [1968] and *Bidaux and Tsang* [1991] are identified as not appropriate for this purpose. A two dimensional fully analytical approach is taken to identify a flow field analogy that allows for determining the properties of a uniform flow field disturbed by an arbitrary number of concentric annular filter rings of arbitrary radii and hydraulic conductivities. Application of this method to the case of a PFM installed in an observation well consisting of a well screen and possible additional filter rings leads to the conclusion that the flow field inside the center circle (PFM sorbent) is always uniform, independently of the number of filter rings and their geometric and hydraulic properties. Furthermore, closed expressions for flow convergence factors are derived for different well configurations and an ad hoc formalism is presented to quickly obtain flow convergence factors for an arbitrary number of filter rings. The resulting flow fields and flow convergence factors show good agreement when validated against numerical solutions. A sensitivity analysis of the flow convergence factors shows that for increasing hydraulic conductivities (e.g., by an order of magnitude) from the aquifer toward the PFM sorbent, uncertainties in the flow convergence factor stemming from uncertainties in the determination of a well screen or aquifer hydraulic conductivity may be significantly reduced.

[43] From one of the convergence relationships, two simple inverse models were derived to facilitate the analysis of PFM data. Both models required unadjusted PFM measures of water flux and data on the depth-averaged aquifer conductivity and the hydraulic gradient. Both models returned estimates of depth-varying aquifer conductivities, from which depth-varying convergence factors and ambient water and contaminant fluxes could be determined. The first model was suitable for the analysis of PFMs installed simple screen wells. Under certain conditions the model would predict depth uniform flow convergence in a stratified aquifer. The second model was formulated for screened

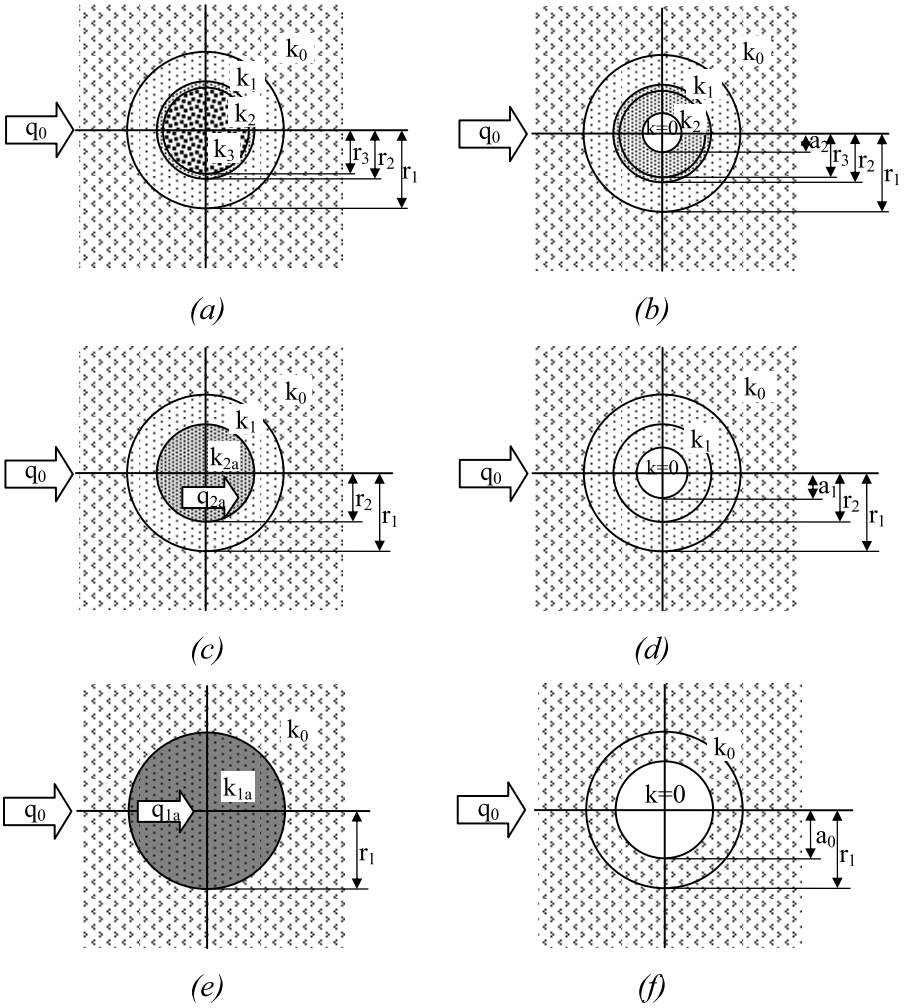

Figure A1. (a–f) Stepwise transformation of flow domain using equations (A1)–(A5) for the derivation of the flow convergence factor.

wells constructed with filter packs. This model predicted depth varying flow convergence under typical field conditions; consequently, this knowledge would be critical in any general assessment of integrated flux or mass flow. Both inverse models were tested using data from a previous field study. Furthermore, both models predicted system conductivity distributions which resulted in subsequent estimates of ambient water and contaminant fluxes that were closely comparable to independent determinations.

Appendix A: Application of the Flow Field Analogy to Determine the Parameters *q* and *a* for Each Filter Ring and the Flow Convergence Factor

[44] Figure A1a represents a cross section of an observation well consisting of a filter pack and a well screen with a PFM installed in it. In order to calculate the flow field in the entire system, the flow field analogy will first be applied in the reverse way as outlined in section 2, namely successively from the center toward the aquifer. This converts the system into a simple impermeable circle in a flow domain of conductivity k_0 with a known solution for the respective flow field as shown in Figure A1. Successive reversing of these initial transformations for every ring going back from the aquifer to the center then provides the solution of the flow field for each ring (Figure A2). The application of the flow field analogy (equations (10) and (11)) to the stepwise transformation of Figure A1 results in the following system of equations.

$$\left(\frac{a_2}{r_3}\right)^2 = \frac{1-\frac{k_3}{k_2}}{1+\frac{k_3}{k_2}} \tag{A1}$$

$$\frac{k_{2a}}{k_2} = \frac{1-\left(\frac{a_2}{r_2}\right)^2}{1+\left(\frac{a_2}{r_2}\right)^2} \tag{A2}$$

$$\left(\frac{a_1}{r_2}\right)^2 = \frac{1-\frac{k_{2a}}{k_1}}{1+\frac{k_{2a}}{k_1}} \tag{A3}$$

$$\frac{k_{1a}}{k_1} = \frac{1-\left(\frac{a_1}{r_1}\right)^2}{1+\left(\frac{a_1}{r_1}\right)^2} \tag{A4}$$

$$\left(\frac{a_0}{r_1}\right)^2 = \frac{1-\frac{k_{1a}}{k_0}}{1+\frac{k_{1a}}{k_0}} \tag{A5}$$

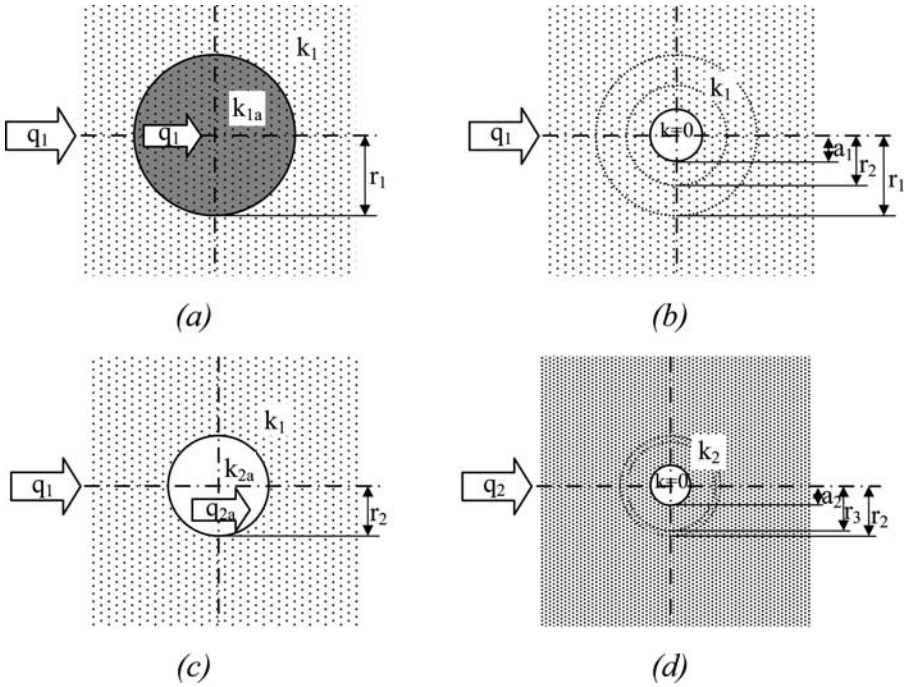

Figure A2. (a–d) Stepwise transformation of the flow domain using equations (A6)–(A10) for the derivation of the flow convergence factor.

[45] In the flow domain of Figure A1f, equation (7) can be applied to express the total flow $\psi_1 = \psi(r_1, \pi/2; q_0, a_0)$ [L^2/T] through the circle of radius r_1 and, subsequently, the uniform flux q_{1a} in Figure A1e.

$$q_{1a} = \frac{\Psi_1}{r_1} = q_0\left[1 - \left(\frac{a_0}{r_1}\right)^2\right] = q_0\frac{2}{1+\frac{k_0}{k_{1a}}} \tag{A6}$$

where equation (A5) is substituted to obtain the last term, which is seen to be equivalent to the flow convergence factor α_1 of equation (3) corresponding to the flow domain of Figure A1e. In Figure A2a, k_0 from Figure A1e is now replaced by k_1, which requires that q_0 be adjusted to q_1 to maintain the same flux q_{1a} inside the circle. Taking advantage of equation (A6) gives

$$q_1 = q_{1a}\frac{1+\frac{k_1}{k_{1a}}}{2} = q_0\frac{2}{1+\frac{k_0}{k_{1a}}}\frac{1+\frac{k_1}{k_{1a}}}{2} = q_0\frac{1+\frac{k_1}{k_{1a}}}{1+\frac{k_0}{k_{1a}}} \tag{A7}$$

[46] By combining the flow domains of Figures A1d and A2a the flow domain of Figure A2b can be generated, which allows for a repeated application of the previous two steps resulting in Figure A2c and

$$q_{2a} = \frac{\Psi_2}{r_2} = q_1\left[1 - \left(\frac{a_1}{r_2}\right)^2\right] = q_0\frac{4}{\left(1+\frac{k_0}{k_1}\right)\left(1+\frac{k_1}{k_{2a}}\right) + \left(1-\frac{k_0}{k_1}\right)\left(1-\frac{k_1}{k_{2a}}\right)\left(\frac{r_2}{r_1}\right)^2} \tag{A8}$$

where equations (A3), (A4), and (A7) are substituted to obtain the last term, which corresponds to the flow convergence factor α_2 of equation (12). Furthermore, q_2 in Figure A2d is obtained as

$$q_2 = q_{2a}\frac{1+\frac{k_2}{k_{2a}}}{2} = q_1\frac{2}{1+\frac{k_1}{k_{2a}}}\frac{1+\frac{k_2}{k_{2a}}}{2} = q_1\frac{1+\frac{k_2}{k_{2a}}}{1+\frac{k_1}{k_{2a}}} \tag{A9}$$

and

$$q_3 = \frac{\Psi_3}{r_3} = q_2\left[1 - \left(\frac{a_2}{r_3}\right)^2\right] = q_0\alpha_3 \tag{A10}$$

where α_3 is the flow convergence factor of equation (13), which is obtained from substituting equations (A1), (A2), (A3), (A4), (A7), and (A9) into equation (A10). Note that for the chosen number of filter rings $q_3 = q_{3a}$ and $k_3 = k_{3a}$. Thus this appendix shows how to determine the parameters q and $\underline{a}$ for each filter ring in order to compute the respective flow fields and how to arrive at respective flow convergence factors for an increasing number of filter rings.

Appendix B: Ad Hoc Formalism to Determine Flow Convergence Factors for an Arbitrary Number of Filter Rings

[47] The method applied in Appendix A is general in a way that the entire flow field can be determined for an arbitrary number of filter rings. However, as to the mere determination of flow convergence factors, inspection of equations (3), (12), and (13) (representing expressions of flow convergence factors for 0, 1 and 2 filter rings, respectively) reveals a particular pattern that is followed in those expressions when a ring is added. This pattern is identified and used herein to present a formalism represent-

$$\left(1+\frac{k_0}{k_1}\right)\cdot\left(1+\frac{k_1}{k_2}\right)\cdot\left(1+\frac{k_2}{k_3}\right)\cdot\left(1+\frac{k_3}{k_4}\right)+$$
$$\left(1-\frac{k_0}{k_1}\right)\cdot\left(1-\frac{k_1}{k_2}\right)\cdot\left(1+\frac{k_2}{k_3}\right)\cdot\left(1+\frac{k_3}{k_4}\right)\cdot\left(\frac{r_2}{r_1}\right)^2+$$
$$\left(1+\frac{k_0}{k_1}\right)\cdot\left(1-\frac{k_1}{k_2}\right)\cdot\left(1-\frac{k_2}{k_3}\right)\cdot\left(1+\frac{k_3}{k_4}\right)\cdot\left(\frac{r_3}{r_2}\right)^2+$$
$$\left(1-\frac{k_0}{k_1}\right)\cdot\left(1+\frac{k_1}{k_2}\right)\cdot\left(1-\frac{k_2}{k_3}\right)\cdot\left(1+\frac{k_3}{k_4}\right)\cdot\left(\frac{r_3}{r_1}\right)^2+$$
$$\left(1+\frac{k_0}{k_1}\right)\cdot\left(1+\frac{k_1}{k_2}\right)\cdot\left(1-\frac{k_2}{k_3}\right)\cdot\left(1-\frac{k_3}{k_4}\right)\cdot\left(\frac{r_4}{r_3}\right)^2+$$
$$\left(1+\frac{k_0}{k_1}\right)\cdot\left(1-\frac{k_1}{k_2}\right)\cdot\left(1+\frac{k_2}{k_3}\right)\cdot\left(1-\frac{k_3}{k_4}\right)\cdot\left(\frac{r_4}{r_2}\right)^2+$$
$$\left(1-\frac{k_0}{k_1}\right)\cdot\left(1+\frac{k_1}{k_2}\right)\cdot\left(1+\frac{k_2}{k_3}\right)\cdot\left(1-\frac{k_3}{k_4}\right)\cdot\left(\frac{r_4}{r_1}\right)^2$$

Figure B1. Comparison of the denominators of equations (3), (12), and (13).

ing an ad hoc alternative to the application of the flow field analogy and allowing for a rapid determination of flow convergence factors for arbitrary numbers of filter rings.

[48] The numerators of equations (3), (12), and (13) are seen to increase by a factor of 2 each time a ring is added, indicating that the numerator of a new flow convergence factor α_4 (dimensionless) will be "16", for example. The denominators are reproduced in Figure B1. The darkly shaded area can be seen to represent the denominator of α_1, while the intermediate shaded area highlights the additional terms to obtain the denominator of α_2 and the lightly shaded area the additional terms to obtain the denominator of α_3. The nonshaded area contains the additional terms that have to be added to the denominator of α_3 to obtain the denominator of α_4. The latter terms can be found by inspection of the changes in the denominators between α_1, α_2 and α_3 and by applying the same pattern once more. The positions of the minuses in the terms of the columns 1 to 4 of Figure B1 are unambiguously defined by the fact that the radius between two adjacent rings has to cancel out if the conductivities of these rings are the same. For example, $1 - k_1/k_2$ is zero for $k_1 = k_2$ and thus all the terms containing r_2 are eliminated from the expression. In the remaining terms, equal conductivities in adjacent rings have to result in a factor "2", since elimination of one ring reduces the numerator to half. For that reason, all the other signs have to be "+". Thus the matrix of Figure B1 may be expanded to any number of additional filter rings.

[49] **Acknowledgments.** This research was supported in part by the DOC Program of the Austrian Academy of Sciences, the Environmental Security Technology Certification (ESTCP) program, U.S. Department of Defense (DOD), project number ER-0114, and the Florida Water Resources Center under a grant from the U S. Department of Interior (067HQGR0079).

References

Annable, M. D., K. Hatfield, J. Cho, H. Klammler, B. Parker, J. Cherry, and P. S. C. Rao (2005), Field-scale evaluation of the passive flux meter for simultaneous measurement of groundwater and contaminant fluxes, *Environ. Sci. Technol.*, *39*, 7194–7201.

Barker, J. F., B. J. Butler, E. Cox, J. F. Devlin, R. Focht, S. M. Froud, D. J. Katic, M. McMaster, M. Morkin, and J. Vogan (2000), *Sequence Reactive Barriers for Groundwater Remediation*, 73 pp., Lewis, Boca Raton, Fla.

Betz, A. (1964), *Konforme Abbildung*, Springer, New York.

Bidaux, P., and C. Tsang (1991), Fluid flow patterns around a well bore of an underground drift with complex skin effects, *Water Resour. Res.*, *27*, 2993–3008.

Bockelmann, A., T. Ptak, and G. Teutsch (2001), An analytical quantification of mass fluxes and natural attenuation rate constants at a former gasworks site, *J. Contam. Hydrol.*, *53*, 429–453.

Borden, R. C., R. A. Daniel, L. E. LeBrun IV, and C. W. Davis (1997), Intrinsic biodegradation of MTBE and BTEX in a gasoline-contaminated aquifer, *Water Resour. Res.*, *33*, 1105–1115.

Devlin, J. F., M. McMaster, and J. F. Barker (2002), Hydrogeologic assessment of in situ natural attenuation in a controlled field experiment, *Water Resour. Res.*, *38*(1), 1002, doi:10.1029/2000WR000148.

Drost, W., D. Klotz, A. Koch, H. Moser, F. Neumaier, and W. Rauert (1968), Point dilution methods of investigating ground water flow by means of radioisotopes, *Water Resour. Res.*, *4*, 125–146.

Dudgeon, C. R. (1967), Wall effects in permeameters, *J. Hydraul. Div. Am. Soc. Civ. Eng.*, *93*, 137–148.

Einarson, M. D., and D. M. Mackay (2001), Predicting impacts of groundwater contamination, *Environ. Sci. Technol.*, *35*, 66A–73A.

Feenstra, S., J. A. Cherry, and B. L. Parker (1996), Conceptual models for the behavior of nonaqueous phase liquids (DNAPLs) in the subsurface, in *Dense Chlorinated Solvents and Other DNAPLs in Groundwater*, edited by J. F. Pankow and J. A. Cherry, pp. 53–88, Waterloo Press, Portland, Oreg.

Halevy, E., H. Moser, O. Zellhofer, and A. Zuber (1967), Borehole dilution techniques—A critical review, in *Isotopes in Hydrology*, pp. 531–563, IAEA, Vienna, Austria.

Harbaugh, A. W., and M. G. McDonald (1996), User's documentation for MODFLOW-96, an update to the U.S. Geological Survey Modular Finite-Difference Ground-Water Flow Model, *U.S. Geol. Surv. Open File Rep.*, *96-485*.

Harlemann, D. R. E., P. F. Mehlhorn, and R. R. Rumer (1963), Dispersion-permeability correlation in porous media, *J. Hydraul. Div. Am. Soc. Civ. Eng.*, *89*, 67–85.

Hatfield, K., M. D. Annable, S. Kuhn, P. S. C. Rao, and T. Campbell (2002), A new method for quantifying contaminant flux at hazardous waste sites, *IAHS Publ.*, *275*, 25–32.

Hatfield, K., M. D. Annable, J. Cho, P. S. C. Rao, and H. Klammler (2004), A direct passive method for measuring water and contaminant fluxes in porous media, *J. Contam. Hydrol.*, *75*, 155–181.

Holder, T., G. Teutsch, T. Ptak, and R. Schwarz (1998), A new approach for source zone characterization: The Neckar Valley study, *IAHS Publ.*, *250*, 49–55.

Kao, C. M., and Y. S. Wang (2001), Field investigation of natural attenuation and intrinsic biodegradation rates at an underground storage tank site, *Environ. Geol.*, *40*, 622–631.

Kearl, P. M. (1997), Observations of particle movement in a monitoring well using the colloidal borescope, *J. Hydrol.*, *200*, 323–344.

King, M. W. G., J. F. Barker, J. T. Devlin, and B. J. Butler (1999), Migration and natural fate of a coal tar creosote plume: 2. Mass balance and biodegradation indicators, *J. Contam. Hydrol.*, *39*, 281–307.

Kubert, M., and M. Finkel (2006), Contaminant mass discharge estimation in groundwater based on multi-level point measurements: A numerical evaluation of expected errors, *J. Contam. Hydrol.*, *84*, 55–80.

Labaky, W. (2004), Theory and testing of a device for measuring point-scale groundwater velocities, Ph.D. thesis, Dep. of Earth Sci., Univ. of Waterloo, Ontario, Canada.

Ogilvi, N. A. (1958), An electrolytical method for determining the filtration velocity of underground waters, *Bull. Sci. Technol. Inf.*, *4*, 1009–1012.

Palmer, C. D. (1993), Borehole dilution tests in the vicinity of an extraction well, *J. Hydrol.*, *146*, 245–266.

Rao, P. S. C., J. W. Jawitz, C. G. Enfield, R. W. Falta, Jr., M. D. Annable, and A. L. Wood (2002), Technology integration for contaminant site remediation: Cleanup goals and performance criteria, *IAHS Publ.*, *275*, 571–578.

Schwarz, R., T. Ptak, T. Holder, and G. Teutsch (1998), Groundwater risk assessment at contaminated sites: A new approach for the inversion of contaminant concentration data measured at pumping wells, *IAHS Publ.*, *250*, 68–71.

Sekhar, G. P., and O. Sano (2000), Viscous flow past a circular/spherical void in porous media—An application to measurement of the velocity of groundwater by the single boring method, *J. Phys. Soc. Jpn.*, *69*, 2479–2484.

Strack, O. D. L. (1989), *Groundwater Mechanics*, Prentice-Hall, Upper Saddle River, N. J.

Strack, O. D. L., and H. M. Haitjema (1981), Modeling double aquifer flow using a comprehensive potential and distribution singularities: 2. Solution for inhomogeneous permeabilities, *Water Resour. Res.*, *17*, 1551–1560.

Teutsch, G., T. Ptak, R. Schwarz, and T. Holder (2000), Ein neues integrales Verfahren zur Quantifizierung der Grundwasserimmission. Teil I: Breschreibung der Grundlagen, *Grundwasser*, *4*, 170–175.

U.S. Environmental Protection Agency (1998), Technical protocol for evaluating natural attenuation of chlorinated solvents in ground water, *Rep. EPA/600/R-98/128*, Washington, D. C.

Wheatcraft, S. W., and F. Winterberg (1985), Steady state passing through a cylinder of permeability different from the surrounding medium, *Water Resour. Res.*, *21*, 1923–1929.

Xie, X. (1994), Solute transport and remediation in the interface zone: Mathematical modelling and field investigation, Ph.D. thesis, 139 pp., Dep. of Earth Sci., Univ. of Waterloo, Ont., Canada.

E. Agyei, K. Hatfield, and H. Klammler, Department of Civil and Coastal Engineering, University of Florida, Gainesville, FL 32611-6450, USA. (khh@ce.ufl.edu)

M. D. Annable, Inter-Disciplinary Program in Hydrologic Sciences, University of Florida, Gainesville, FL 32611-6450, USA.

J. A. Cherry and B. L. Parker, Department of Earth Sciences, University of Waterloo, Waterloo, ON Canada N2L 3G1.

P. S. C. Rao, School of Civil Engineering, Purdue University, West Lafayette, IN 47907, USA.